Study on the Influence of Lattice Integrity and Phase Composition to the Photocatalytic Efficiency of ZnS Material

--Supplementary Material

Yangping Hong,[a] Zhang Lin,[b] Jin Huang,[a] Yongjing Wang,[b,]* and Feng Huang[a,]*

Key Laboratory of Optoelectronic Materials Chemistry and Physics, Fujian Institute of Research on the Structure of Matter, Chinese Academy of Sciences, Fuzhou, Fujian, 350002, China

*Corresponding author: yjwang@fjirsm.ac.cn, fhuang@fjirsm.ac.cn,

1. Experimental details.

The preparation of original ZnS microsphere. All chemicals were AR reagents from Sinopharm Medicine Company without further purification. The original ZnS microsphere was synthesized by hydrothermal method as reported in our previous work[1]. In details, ZnO (0.167 g, 2 mmol) was dissolved in a mixture of NaOH (16 M, 12.875 ml) and Na_2S (1 M, 2 ml). It was then put into a hydrothermal bomb that was sealed and heated at 230 □ for 12 h. The bomb was forcedly cooled to room temperature rapidly after heat treatment. The white powder was filtered and washed with excess water and absolute ethanol, and finally dried in air at room temperature for 8 h.

The annealing treatments. The obtained ZnS nanomicrosphere was then annealed for analyzing the effects of different anneal situations on the photocatalytic efficiency of ZnS. For each vacuum annealing treatment, 30 mg ZnS was put into a quartz tube, sealed when the vacuum pressure of the tube arrived at 10^{-3} Pa, and then annealing at appropriate temperature for certain time in tube furnace.

Photocatalytic performances: Before photocatalytic experiment, the as-synthesized ZnS need to be acidification treated to eliminate the -OH quenching center on the crystal surface[2]. Photochemical degradation was carried out in self-designed stainless steel (capacity ca. 100 mL). The reaction system containing eosin B ($C_{20}H_6Br_2N_2Na_2O_9$; 5.0×10^{-5}M 50 mL) and ZnS catalyst (10 mg) was magnetically stirred in the dark for 15 min to reach the adsorption equilibrium of eosin B with the catalyst, and then exposed to UV light from a Philips HPK high-pressure Hg lamp (125 W). After 30 min's irradiation, the mixture was separated by centrifugation and the concentration of the solution is measured by UV–Vis adsorption spectra.

Instruments. X-ray diffraction (XRD) was used to identify the phase composition and average particle sizes of initial and coarsened samples. Diffraction data were recorded using a PANalytical

X'Pert PRO diffractometer with Cu KR radiation 40 kV, 40 mA) in the step scanning mode. The 2θ scanning range was from 15°to 65° in steps of 0.02° with a collection time of 35 s per step. Scanning electronic microscopy (SEM) analyses were used to confirm the particle size and to determine the particle morphology. Samples were prepared for SEM study by dispersing the ZnS powder onto a holey carbon-coated support. The SEM analyses were performed using a JSM-6700F instrument. High-resolution transmission electron microscopy (HRTEM) was used to determine the morphology and detailed microstructure and phase identification of individual particles. Samples were prepared for HRTEM study by dispersing the ZnS powder onto 200-mesh carbon-coated copper grids. HRTEM analyses were performed using a JEOL JEM2010 HRTEM instrument at 200 kV. The nitrogen adsorption and desorption isotherms at 77 k were measured using a Micrometrics ASAP 2020 system after the sample was degassed in vacuum at 120 ^{o}C overnight. A shimadzu UV-2550 spectrophotometer was used to record the UV/Vis spectra of various samples.

2. Control experiments for photodegradation of eosin B.

Fig. S1 shows the control experiments for photodegradation of eosin B. As illustrated by Fig.S1-b, the degradation process of eosin B solution containing original ZnS microsphere catalyst follows the first-order kinetics, which is consistent with Ref. 5. To facilitate comparison, we use half-life period to characterize the photocatalytic efficiency of ZnS under different treatment conditions. The half-life period could be calculated as follows：

$$T_{1/2} = \frac{t \ln 2}{\ln \frac{C_0}{C}} \quad (1)$$

where C_0 is the initial concentration, C is the concentration after a given treatment, t is the reaction time, and $T_{1/2}$ is half-life period.

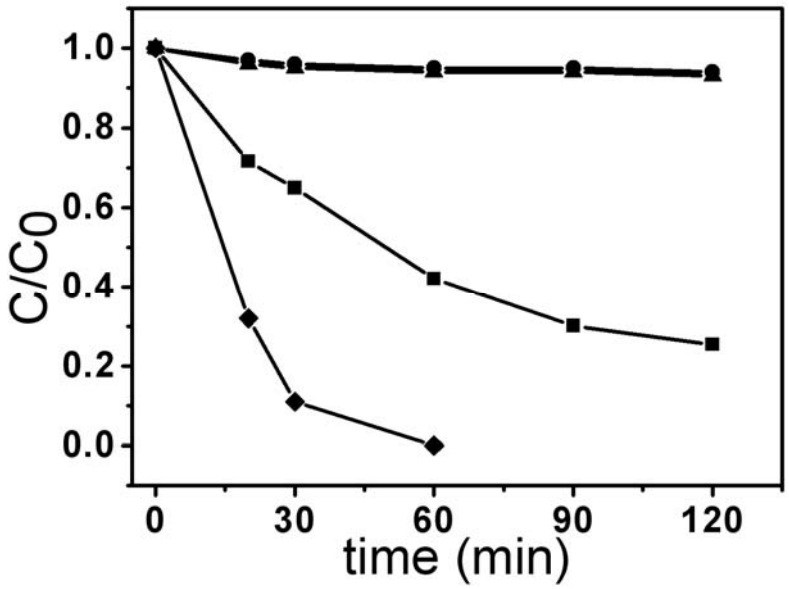

(a)

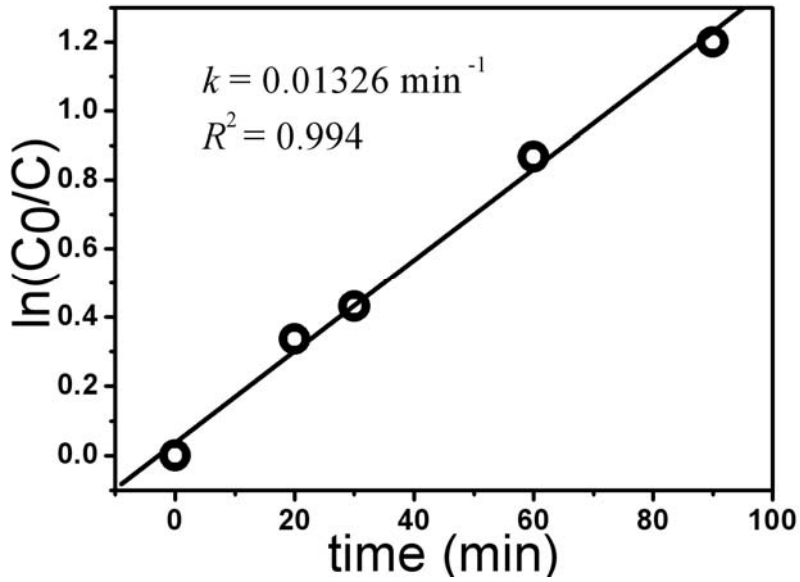

(b)

Fig S1 (a) Photodegradation of eosin B (5.0×10^{-5} M, 50 ml) with 10 mg different kinds of catalyst: ● in the UV light only, ▲ in the dark with original ZnS microsphere, ■ in UV light with original ZnS microsphere, ◆ in the UV light with Degussa P25; **(b)** the liner fit of degradation process of eosin B solution containing the original ZnS microsphere.

3. The calculation of the phase composition and average size of ZnS samples.

Because of the close similarity in the structures of sphalerite and wurzite, many strong XRD peaks overlap. The phase composition of each sample can be calculated from the integrated intensities of the

wurtzite (100) peak (2θ=27.01) and the overlapping sphalerite (111) and wurtzite (002) peaks (2θ=28.64) as illustrated in literature[4]. If the intensity ratio of wurtzite (100) to the overlapping peak is R, then the weight fraction of wurtzite (X_w) can be calculated as

$$X_w = \frac{R}{I_w I_{ws} - R(I_{ws}\text{-}1)} \quad (2)$$

Where I_w = 3.88 represents the intensity ratio of the wurtzite (100) peak to the (002) peak, and I_{ws} = 0.491 is the intensity ratio of the wurtzite (002) peak to the sphalerite (111) peak.

The decomposition of sphalerite and wurtzite peaks overlapping is fitted by using PersonVII program, as shown in Fig. S2.

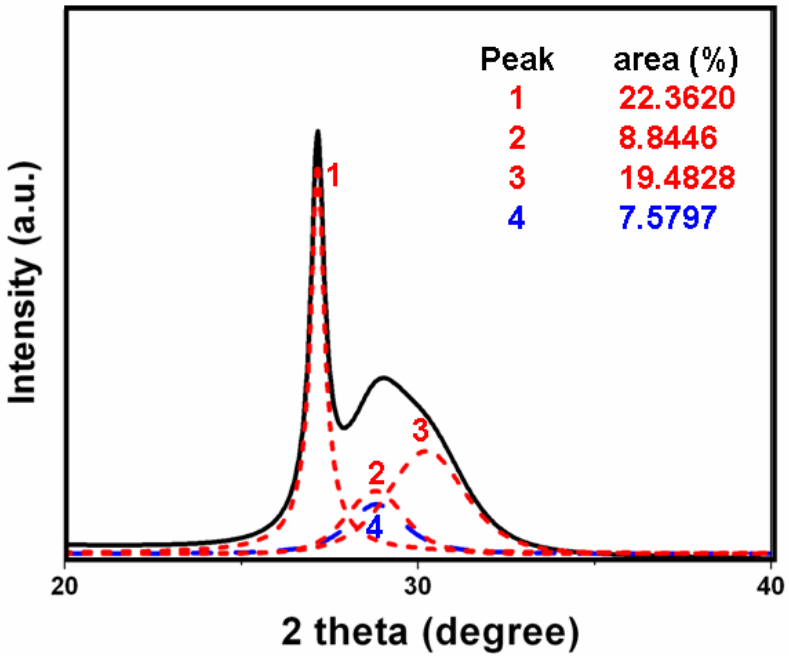

Fig. S2 the decomposition of the sphalerite and wurtzite peaks overlapping of the original ZnS microsphere. The red refer to the (100), (002) and (101) peaks of the wurtzite and the blue refer to the (111) peak of spharelite. The wurtzite phase content calculated according to Ref. 4. is 52%.

The average crystallite size was calculated from the peak broadening using the Scherrer equation[3]

$$D = \frac{0.90\lambda}{\text{fwhm}\cos\theta} \quad (3)$$

Where λ is the wavelength of Cu KR radiation (1.5418 Å), 0.90 is the Scherrer constant, θ is the Bragg reflection angle, and fwhm is the full width at half-maximum intensity of the chosen XRD peak.

4. The structure of the nanosheet in the original ZnS microsphere.

TEM observations were implemented to investigate the phase of the nanosheets in the original ZnS microsphere. The nanosheets were ultrasonically exfoliated from the microspheres for the observation of the open face of the sheet (Fig. S3-a,b). Close inspection of the HRTEM image shows that the nanosheet phase exhibits w[100] close packing. But it is subdivided into domains of incoherent lattice orientations. Lattice distortion can also be clearly observed.

In order to observe the side face of the nanosheet, the sheets were cut using an ultramicrotome (Leica EM UC6), and ultrathin sections were obtained (Fig. S3-c, d). It shows that the thickness of the sheet is 10 ~ 20 nm. The HRTEM image shows that the side face of the nanosheet exhibits w[001] close packing. Combining with the XRD data, it can be conclude that the original microsphere is made up of 10 ~20 nm thick wurtzite nanosheets.

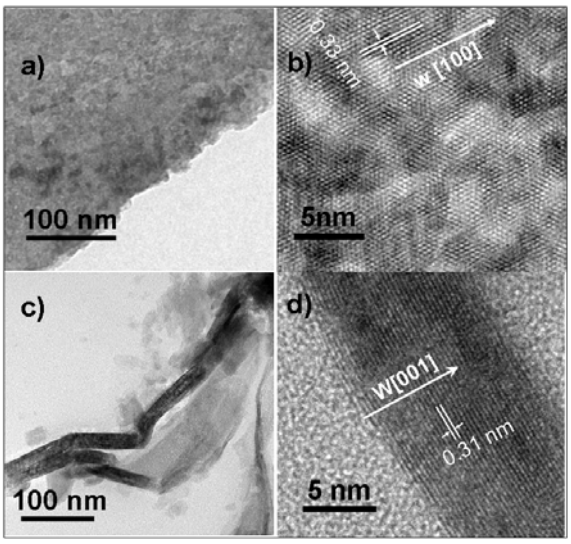

Fig. S3. **(a)** The TEM image of the nanosheet shed from the ZnS microshpere; **(b)** The HRTEM image of the nanosheet which shows w[100] close packing; (c) The TEM image of ultrathin sections cut from the nanosheets ; (d) The HRTEM image of an ultrathin section which shows the close packing along w[001].

5. The structure of the Sphalerite $S_{200\text{-}45min}$

The microspheres of **$S_{200\text{-}45min}$** were ultrasonically treated for the TEM observation of the fine structure of the microsphere. As shown in Fig. S4, the size of nano particles which were exfoliated from the microsphere ranges from 10 ~ 20 nm, which is consistent with the XRD and SEM data. Both SEAD pattern and HRTEM image indicate that the phase of particles is sphalerite.

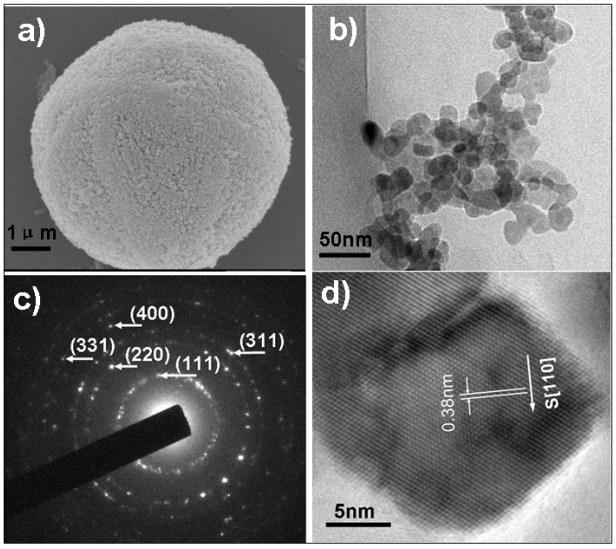

Fig. S4. (a) SEM image of the ZnS microsphere of $S_{200\text{-}45min}$; (b) TEM image of the sphalerite particle exfoliated from the microsphere; (c) SEAD pattern of the sample shown in (b); (d) The HRTEM image of a individual particle of the microsphere.

6. The structural evolution of the ZnS microsphere during the moderate annealing process.

Fig. S5 shows the structural evolution of the ZnS micorsphere during the moderate heating process. The architecture of the nanosheet in the original microsphere can be interpreted as the connection of pieces of wurtzite ZnS particles with the lattice distortion and the deorientation of the domains in the sheet.

If the original ZnS microspheres are annealed at 150 °C for not over 3 hours, the major change in the structure of the nanosheet is the lattice rearrangement while the phase and morphology unchanged. The annealing process will lead to an increase of the crystal integrity. If the microspheres are heated over a longer time or at a relative higher temperature (200 °C), it will result in a phase transformation from wurzite to sphalerite and a crash of the nanosheet. After phase transformation, the size of the spalerite is similar to that of the wurtzite of original microsphere.

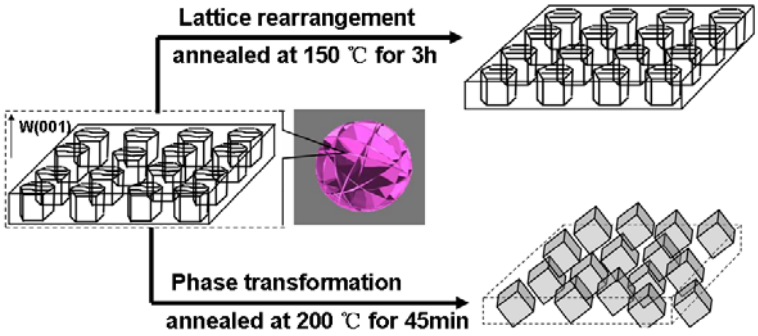

Fig. S5. The schematic diagram of the structural evolution of the ZnS microsphere.

7. The interpretation about the influence of the phase composition to the photocatalytic activity

The conclusion that the phase transition can lead to an increase in the photocatalytic activity could be drawn from the series data of the samples annealed at 150 ^{o}C. As shown in the text, the crystal integrity of original ZnS (S_0) has been increased greatly after it is annealed for 2 h at 150 ^{o}C. In the annealing period from 2 to 3h, the phase and size are still not changed, however, the crystal integrity changes little in this period (degradation HLP (half-life period) of $S_{150\text{-}2h}$ is 22.5 min and that of $S_{150\text{-}3h}$ is 21.8 min). This ***indicates the extending of the annealing time over 3 h will have very little influence to the crystal integrity.*** However, during experiment, we found when the annealing time extend to 5h and 10h, the photocatalytic efficiency of the material further increase obviously (The degradation HLP drops from $S_{150\text{-}3h}$'s 21.8 min to $S_{150\text{-}10h}$'s 17.8 min). Since in this time period, the phase transition from wurtzite to sphalerite occurs, thus it is quite reasonable for us to attribute the increase of the photocatalytic activity to the change of the phase composition.

At relative higher temperature (200 ^{o}C), the rate of phase transition is fast. During the annealing period from 0 to 45 min, the wurtzite content has dropped from 52% to 3%, meanwhile, the variation of the crystal integrity may be involved in this process. However, the increase of the photocatalytic efficiency caused by the structural evolution in this annealing process (the degradation HLP drops to $S_{200\text{-}45min}$ 10.3 min) is much greater than that solely caused by the enhancement of the crystal integrity in the annealing process at 150 ^{o}C (the degradation HLP of $S_{150\text{-}3h}$ is only 21.8 min). Combine with the above conclusion that the phase transition can lead to an obvious increase in the photocatalytic activity, the increase of the catalytic activity at higher temperature (200 ^{o}C) could be mainly attribute to the change in the phase composition.

1. D. S. Li, Z. Lin, G. Q. Ren, J. Zhang, J. S. Zheng and F. Huang, *Cryst. Growth. Des.*, 2008, **8**, 2324-2328.
2. D. S. Li, F. Huang, G. Q. Ren, Z. Y. Zhuang, D. M. Pan and Z. Lin, *J. Nanosci. Nanotechno.*, 2009, **9**, 6721-6725.
3. R.Jenkins and R. L. Snyder, *Introduction to X-ray Powder Diffractometry*, John Wiley & Sons, New York, 1996; p 90.
4. F. Huang and J. F. Banfield, *J. Am. Chem. Soc.*, 2005, **127**, 4523-4529.
5. J. S. Hu, L. L. Ren, Y. G. Guo, H. P. Liang, A. M. Cao, L. J. Wan and C. L. Bai, *Angew. Chem., Int. Ed.*, 2005, **44**, 1269-1273.